The American Journal of Human Genetics, Volume *104*

Supplemental Data

Lack of *GAS2L2* Causes PCD by Impairing Cilia Orientation and Mucociliary Clearance

Ximena M. Bustamante-Marin, Wei-Ning Yin, Patrick R. Sears, Michael E. Werner, Eva J. Brotslaw, Brian J. Mitchell, Corey M. Jania, Kirby L. Zeman, Troy D. Rogers, Laura E. Herring, Luc Refabért, Lucie Thomas, Serge Amselem, Estelle Escudier, Marie Legendre, Barbara R. Grubb, Michael R. Knowles, Maimoona A. Zariwala, and Lawrence E. Ostrowski

SUPPLEMENTAL DATA

SUPPLEMENTAL FIGURES

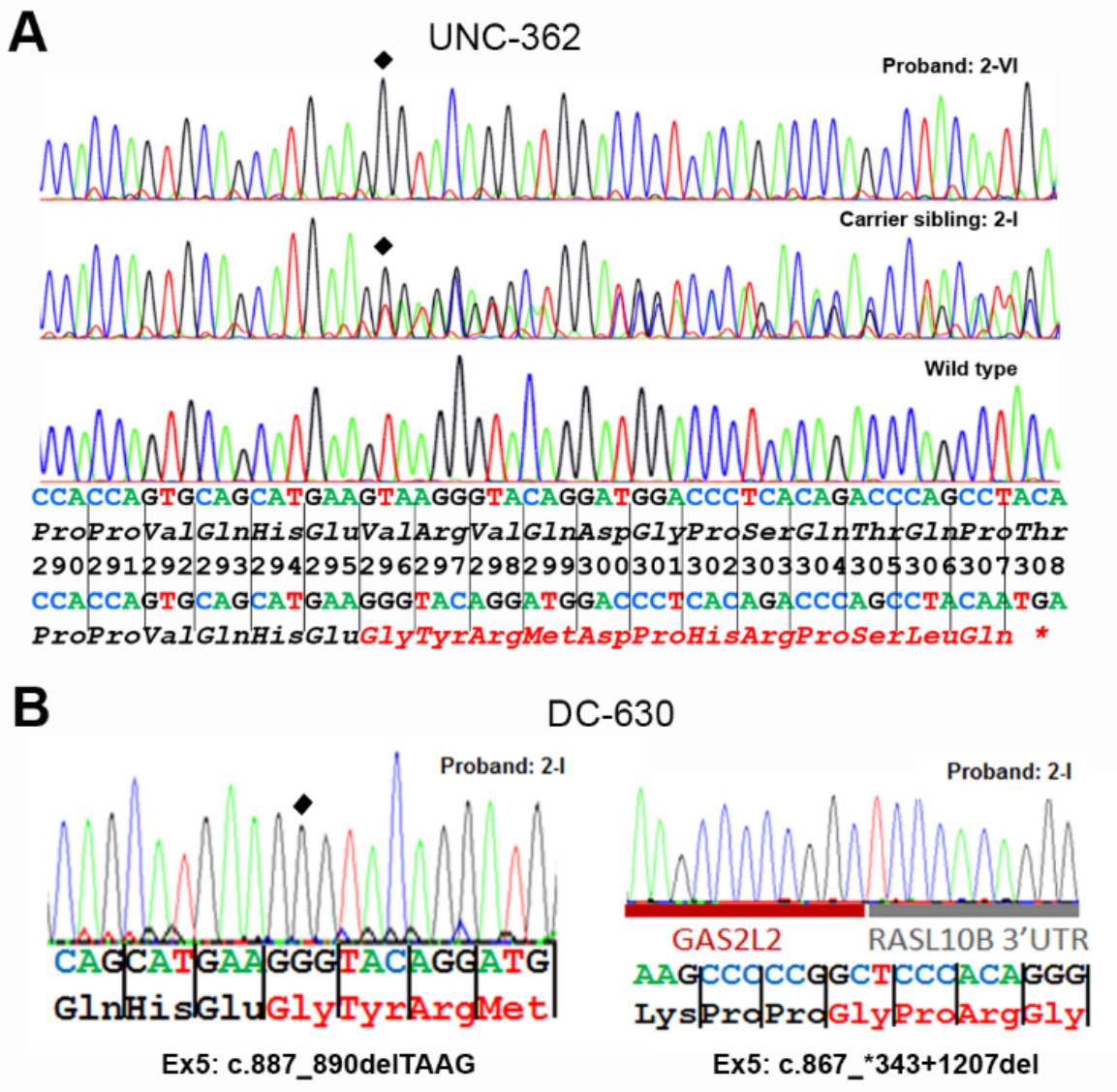

Figure S1: Sanger sequencing of pathogenic genetic variants discovered in *GAS2L2*.
(A) Sequencing of pathogenic variant [c.887_890delTAAG (p.Val296Glyfs*13)] in exon 5 of *GAS2L2* (NM_139285.3, Chr.17q12) in affected subject PCD-1367 (2-IV) of family UNC-362, (top), heterozygous (middle) and wild type (bottom). The variant (filled diamond) induces a frameshift in the gene sequence leading to a stop codon in amino acid 308 during translation.
(B) Sequencing of compound heterozygous variants [c.[887_890del];[867_*343+1207del], p.[(Val296Glyfs*13)] ;(0?)] in exon 5 of *GAS2L2* in affected subject DCP-1040 of family DC-630, proband 2-1. As both deletions overlap, c.887_890del was seen as hemizygote; allele *in trans* of 867_*343+1207del was not co-amplified because of higher amplicon size (3,931 bp compared to 267 bp for the 867_*343+1207del allele PCR product). Base sequences, amino acid sequences, and codon numbers are shown. Mutated amino acids are represented by red fonts.

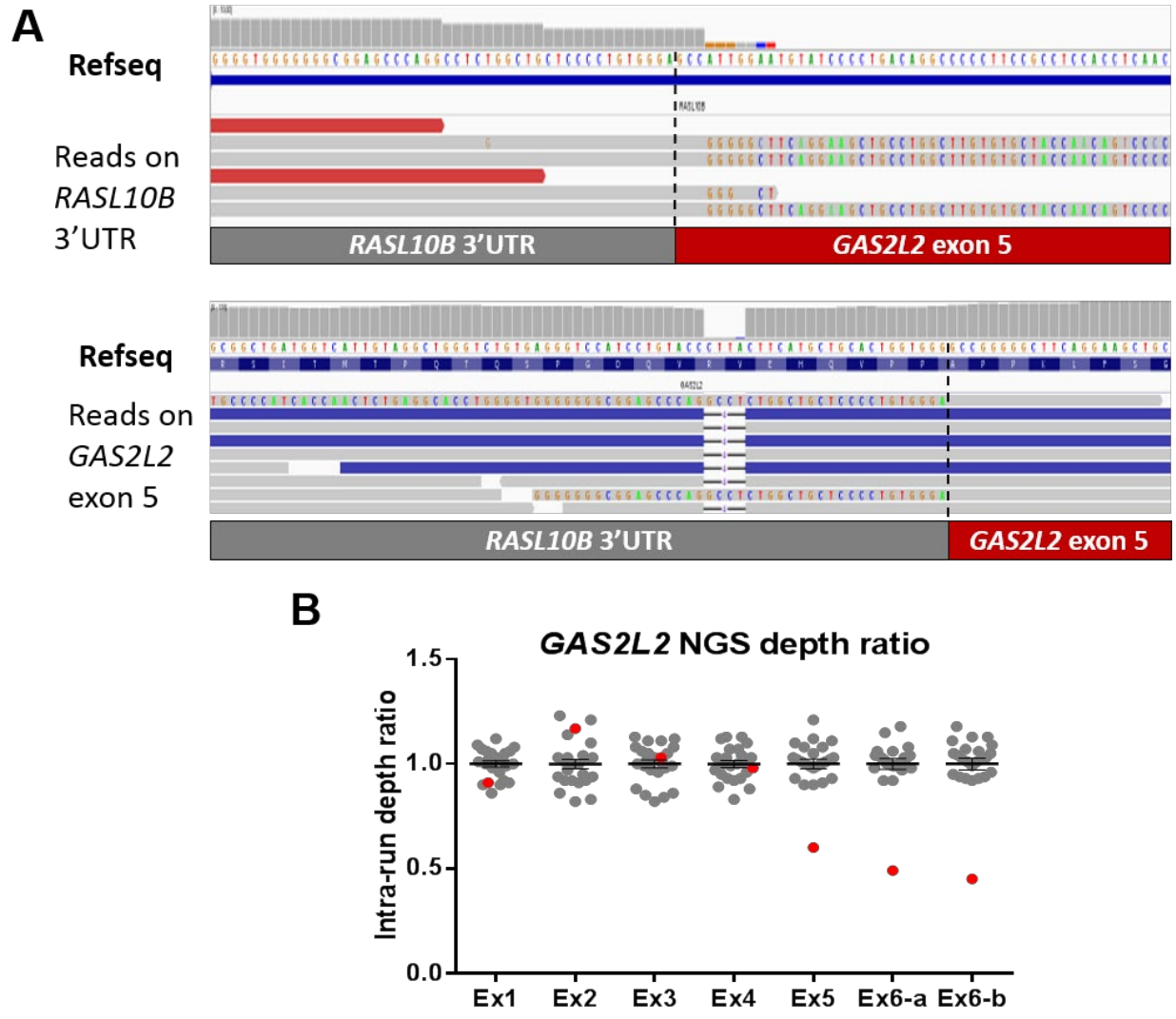

Figure S2: Proband DCP-1040 is an obligatory compound heterozygous.
(A) Breakpoints of the c.867_*343+1207del large deletion (3,931 nucleotides) in *GAS2L2*. Panels show overlapping read sequences aligned on *RASL10B* (upper) or *GAS2L2* (lower). The 5'-breakpoint localizes within *GAS2L2* exon 5 and 3'-end is within the 3'UTR of *RASL10B*. The lower panel also shows 7 reads encompassing the 4-nucleotide c.887_890del *GAS2L2* deletion, which demonstrates the compound heterozygous genotype. Parallel sequencing data are shown as not reverse-complemented in the IGV viewer.
(B) *GAS2L2* copy-number variation analysis in subject DCP-1040 by parallel sequencing depth ratio analysis. Plot shows normalized depth ratio for 24 subjects analyzed within the same run. Mean depth for each capture probe was first normalized for each subject against the contribution of each subject to the run global depth. For each probe, the mean of the normalized depth ratio was calculated and adjusted to 1. Each point corresponds to the depth ratio of each controls (n= 23 grey symbols) or subject DCP1040 (red symbols). Error bars show the standard error of the mean. Exon 6, which is a large exon, was captured by two probes (Ex6-a and Ex6-b). Data highlight a heterozygous loss of most of exon 5 and entire exon 6.

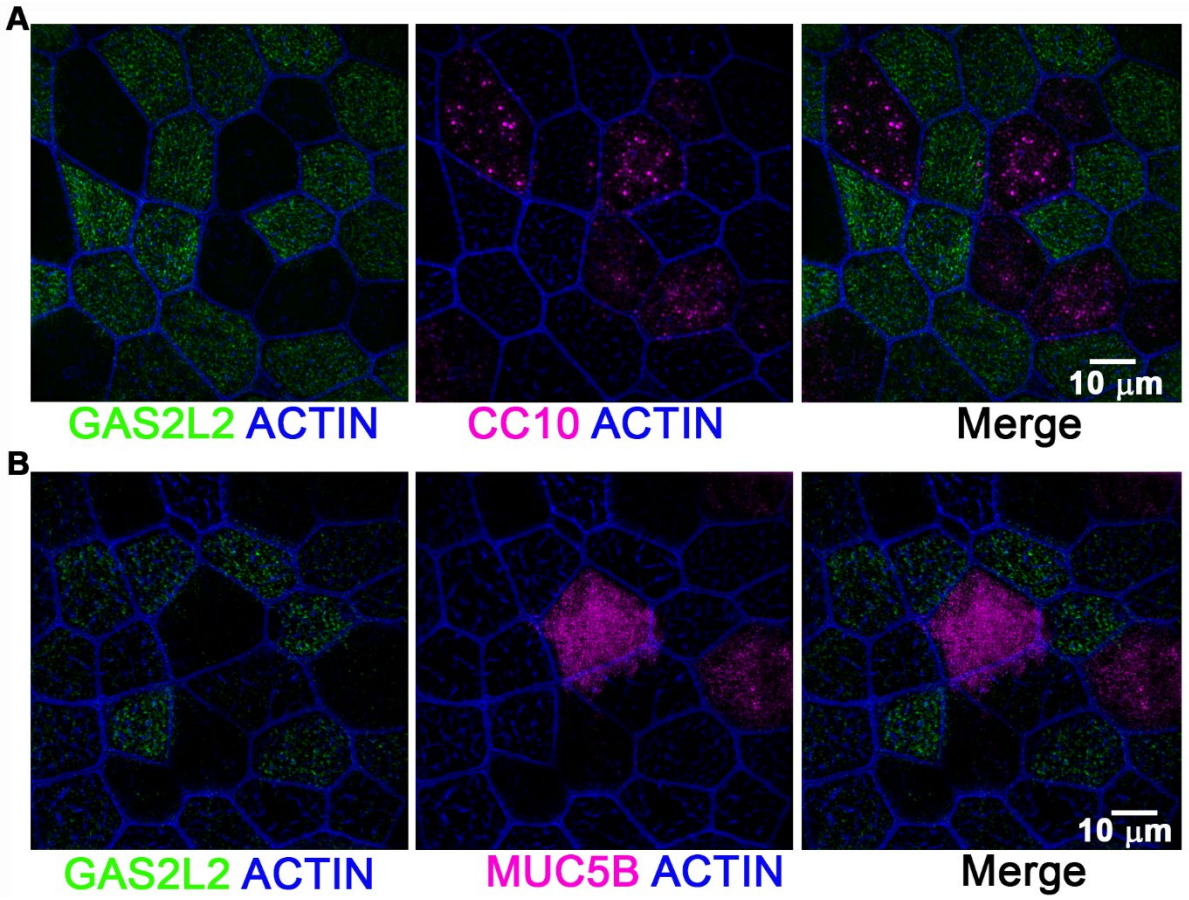

Figure S3: GAS2L2 is not expressed in airway secretory cells: Normal HBE cell were cultured at ALI and whole cultures were stained for GAS2L2 (green) and A) CC10, a club cell specific marker (n=3) or B) MUC5B a goblet cell specific marker (n=3).

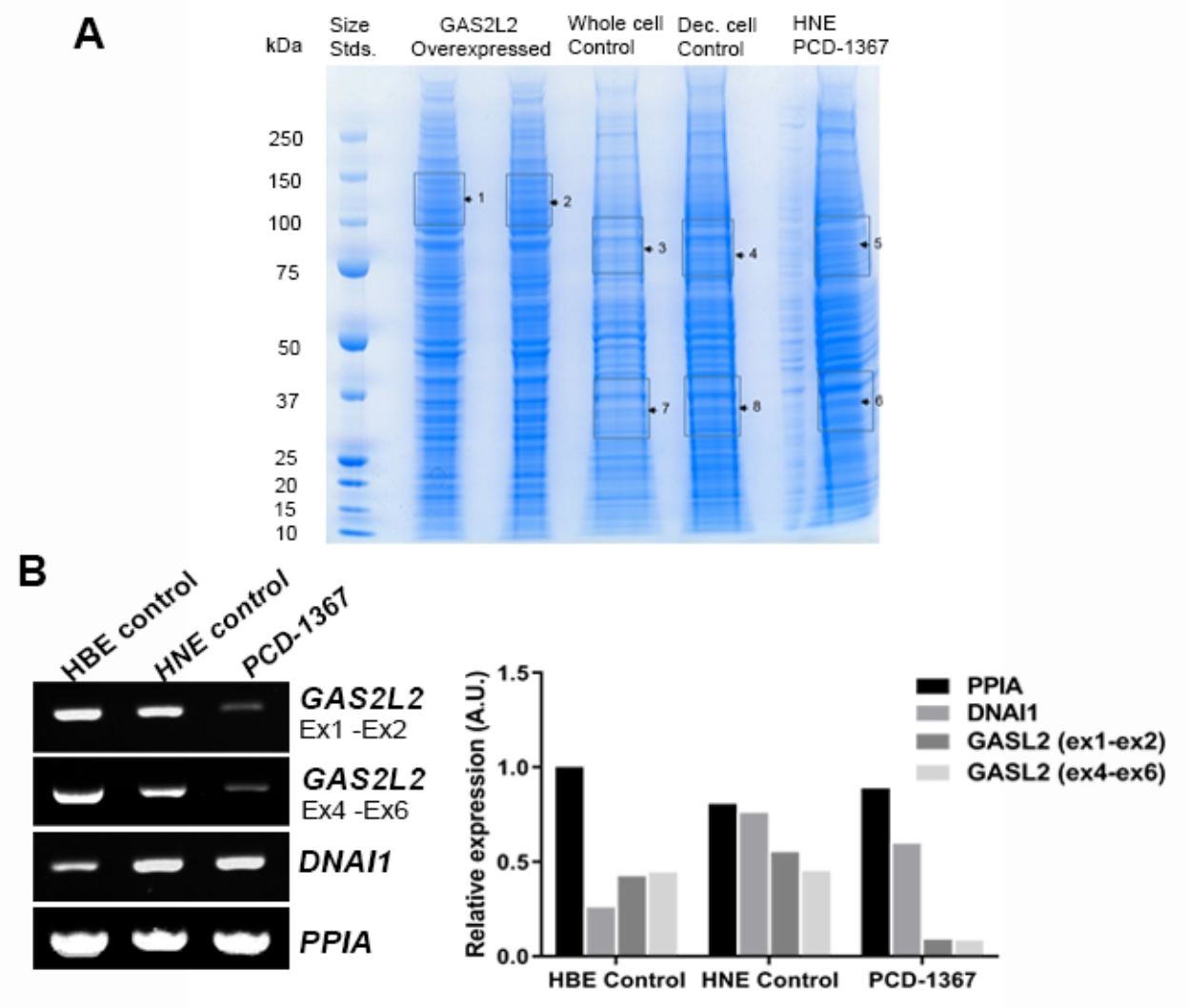

Figure S4: Detection of *GAS2L2* in HNE cells from subject PCD-1367.
(A) Separation of proteins for GAS2L2 targeted proteomics analysis. Proteins were separated on a 4-12% gradient polyacrylamide gel as described in supplementary methods and stained with Coomassie blue to visualize proteins. The gel was cut into the boxed sections for analysis by mass spectrometry.
(B) Total RNA was isolated from cultured control HBE cells, control HNE cells, and PCD HNE cells (PCD-1367). RT-PCR and corresponding normalization confirmed decreased expression of *GAS2L2* in PCD HNE cells.

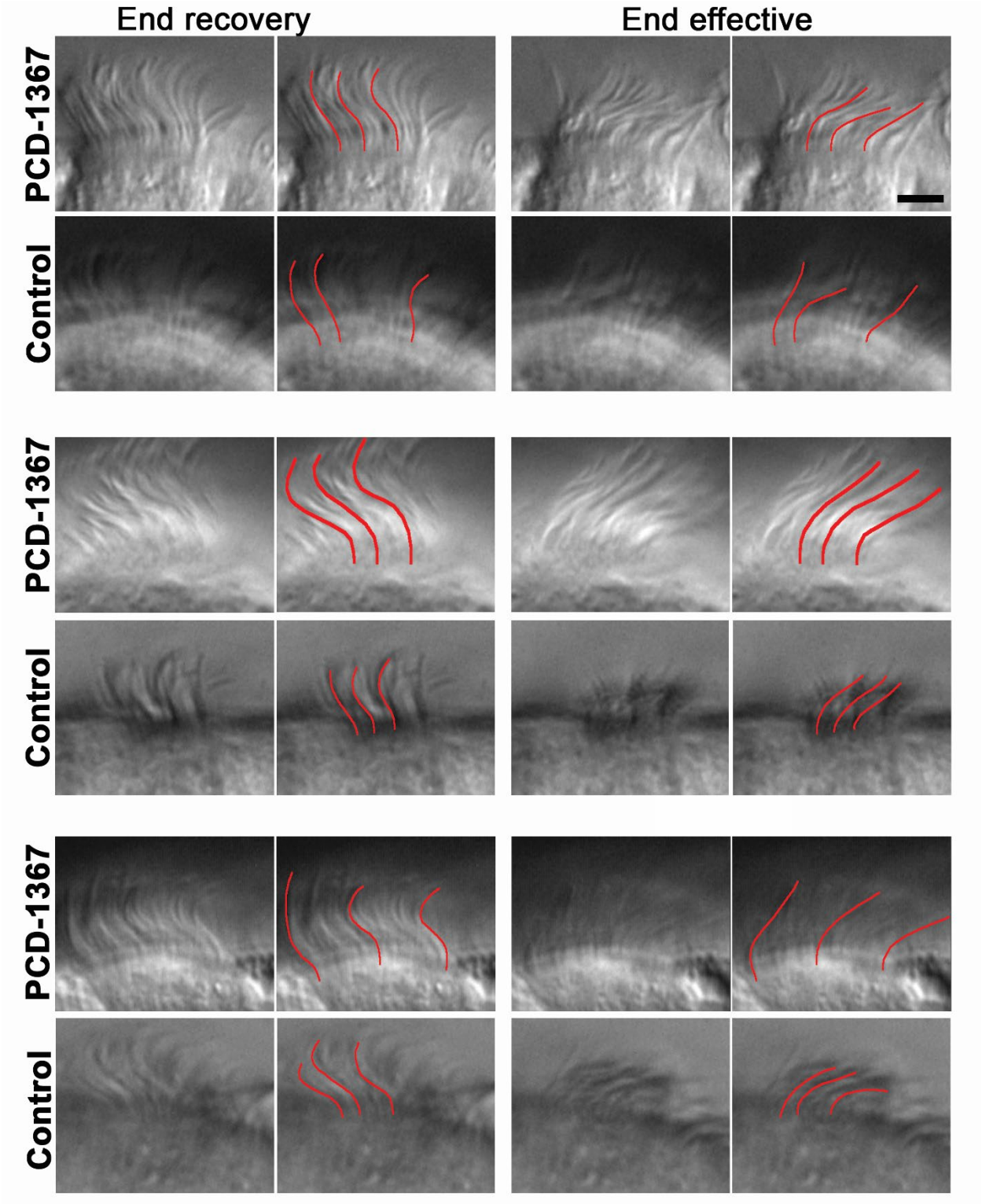

Figure S5: Normal waveform of ciliary beat in *GAS2L2* deficient cells. High-resolution videos of control and PCD ciliated cells were observed and the waveform was traced manually. The images represent a time point of the cilia seen in profile during the end recovery (left panels) and end effective positions (right panels). For each stroke position, a panel highlighting the cilia in red is shown. Scale bar, 4 μm.

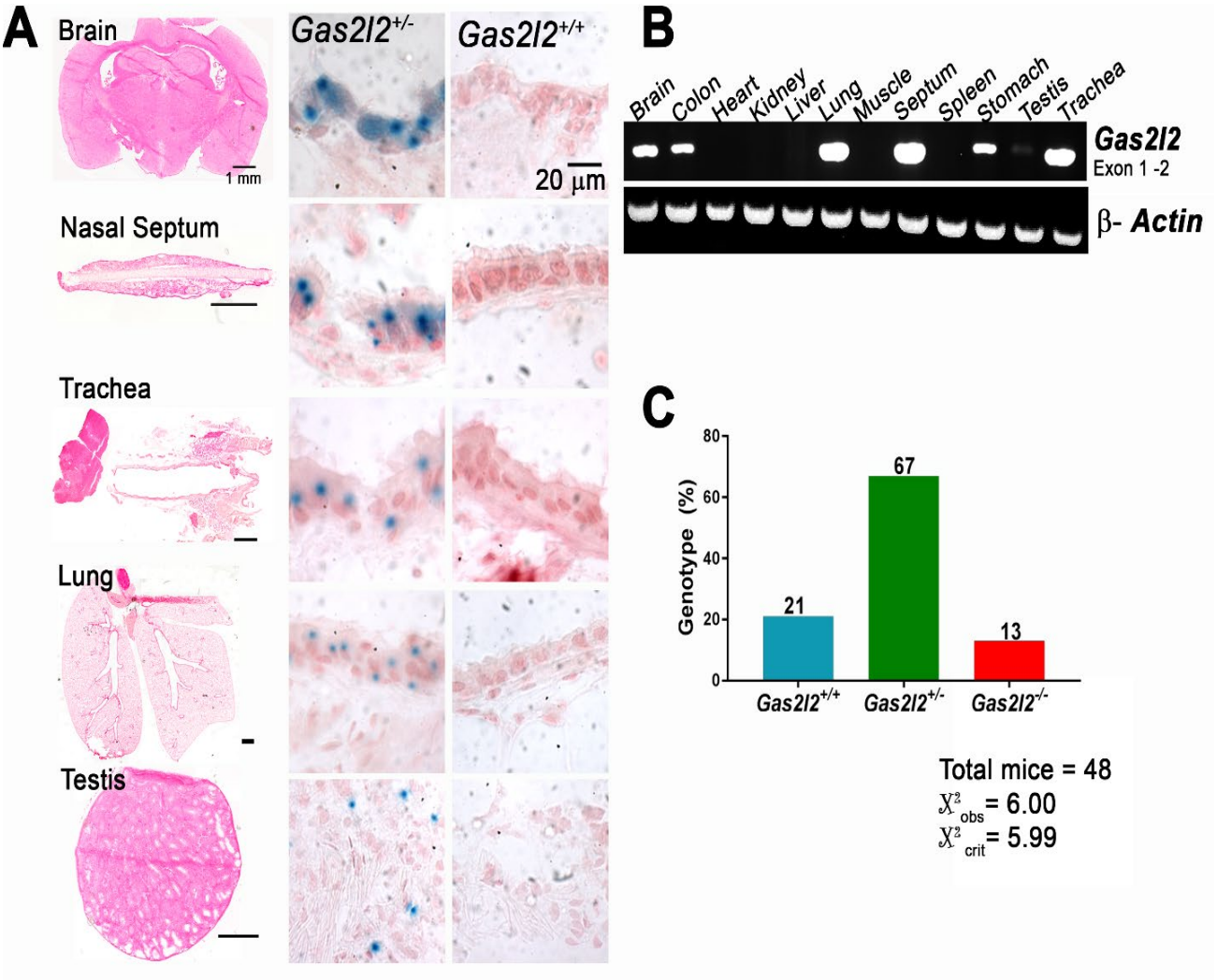

Figure S6: Expression of *Gas2l2* in mouse tissue and the effects of lack of *Gas2l2* on Mendelian distribution.

(A) β-galactosidase staining of different mouse tissue. The whole tissue section is shown in the left panel. Positive β-galactosidase staining was observed in tissues from *Gas2l2*$^{+/-}$ mice carrying the *LacZ* reporter (middle panel). No staining was observed in *Gas2l2*$^{+/+}$ mice (negative control, right panel).

(B) Total RNA from different mouse tissues was extracted and the expression of *Gas2l2* was evaluated by RT-PCR. Reference, *β-Actin*.

(C) Inheritance ratio in *Gas2l2*$^{+/-}$ cross follows Mendelian distribution.

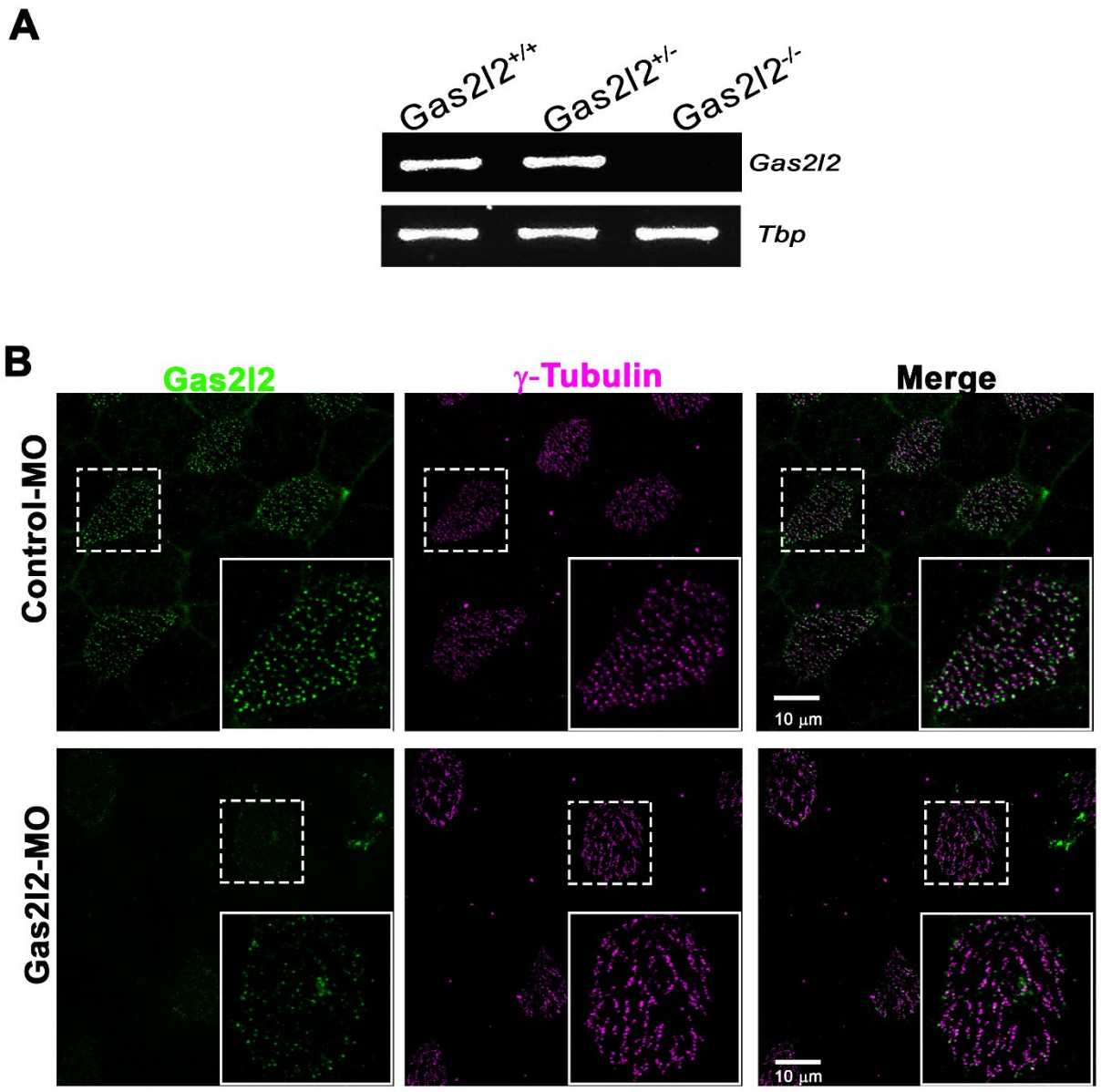

Figure S7: Confirmation of the absence of Gas2l2.
(A) Total RNA was isolated from embryonic mTEC cultures. RT-PCR confirmed the absence of *Gas2l2* expression in *Gas2l2*$^{-/-}$ cultures.
(B) Immunofluorescence of *X. laevis* embryos stained for Gas2l2 (green) and γ-Tubulin to visualize basal bodies (magenta). *X. laevis* embryos treated with *Gas2l2*-MO had reduced positive staining for Gas2l2.

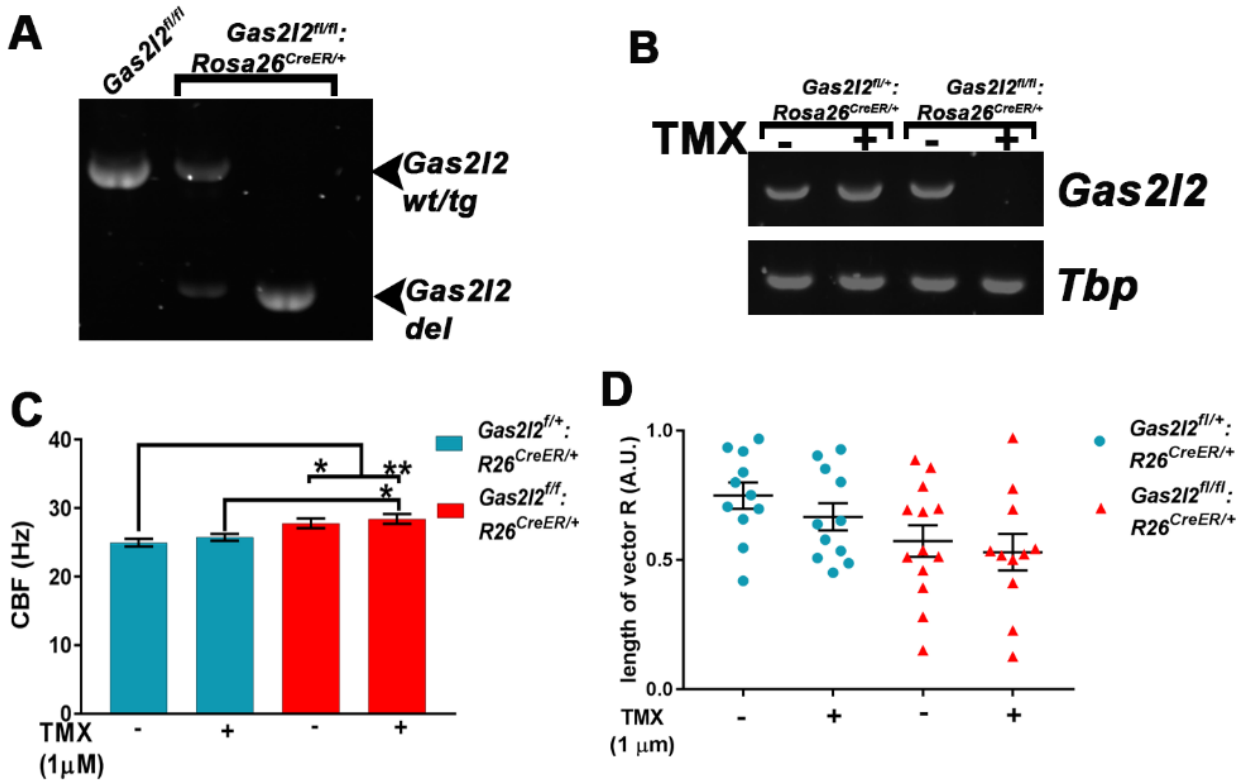

Figure S8: mTEC cultures from *Gas2l2*$^{-/-}$:*R26*$^{CreER/+}$ mice had affected ciliary beat and orientation.
(A) RT-PCR confirmed the spontaneous deletion of *Gas2l2* in *Gas2l2*$^{-/-}$:*R26*$^{CreER/+}$ mice. Mice with 100% deletion did not survive.
(B) The deletion of *Gas2l2* in mTEC cultures treated with tamoxifen (TMX) was corroborated by RT-PCR.
(C) The CBF in *Gas2l2*$^{-/-}$:*R26*$^{CreER/+}$ mTEC cultures treated with TMX was hyperkinetic compared to control (n = 3 biological replicates, 3 technical replicates each. ** p = 0.0019, * p < 0.05).
(D) The orientation of basal body-basal foot was scored in EM images. The length of the vector (0< R <1) for each cells is represented in the graph. The average length of the vector was shorter in *Gas2l2*$^{-/-}$ *:R26*$^{CreER/+}$ ciliated cells treated with TMX compared to control cells.

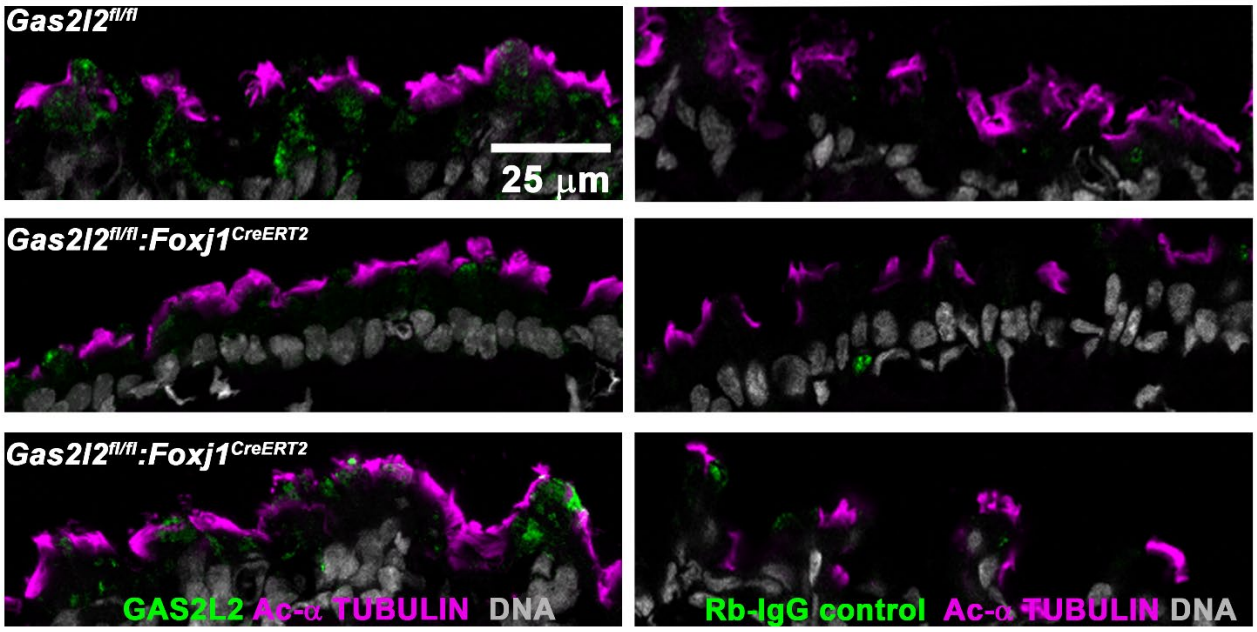

Figure S9: Confirmation of partial deletion of *Gas2l2*. Trachea sections of control and *Gas2l2* conditional-KO mice treated with TMX were stained for GAS2L2 (green), Acetylated- α TUBULIN (magenta), and DNA (gray) (left panels). In the *Gas2l2* conditional-KO two patterns of staining were observed: mice with reduced positive staining for GAS2L2 (middle panel) and mice with close to normal positive staining (bottom panel). The corresponding negative control using anti-rabbit-IgG is shown (right panels).

Table S1: Genes, implicated in PCD, analyzed by targeted capture parallel sequencing

Gene	References*
ARMC4	Zariwala, M.A., Knowles, M.R., and Leigh, M.W. (2007 [Updated 2015]). Primary Ciliary Dyskinesia. In GeneReviews(R), R.A. Pagon, M.P. Adam, H.H. Ardinger, S.E. Wallace, A. Amemiya, L.J.H. Bean, T.D. Bird, N. Ledbetter, H.C. Mefford, R.J.H. Smith, et al., eds. (Seattle (WA), University of Washington, Seattle; 1993-2017[1]
C21ORF59	
CCDC39	
CCDC40	
CCDC65	
CCDC103	
CCDC114	
CCDC151	
CCNO	
DNAAF1	
DNAAF2	
DNAAF3	
DNAAF4	
DNAAF5	
DNAH5	
DNAH11	
DNAI1	
DNAI2	
DNAL1	
DRC1	
DYX1C1	
HYDIN	
LRRC6	
MCIDAS	
NME8	
RPGR	
RSPH1	
RSPH3	
RSPH4A	
RSPH9	
SPAG1	
ZMYND10	
C11ORF70	Höben I. M. et al 2018[2] and Fassad et al 2018[3]
DNAJB13	El Khouri E. et al 2016[4]
GAS8	Olbrich H. et al 2015[5]
LRRC56	Bonnefoy S. et al 2018[6]
PIH1D3	Olcese C. et al 2017[7] and Paff T. et al 2017[8]
STK36	Edelbush C. et al 2017 [9]
TTC25	Wallmeier J. et al 2016[10]

(*) References also listed in the main text

TableS2: Primer sequences for PCR amplification of genomic DNA for all of the six coding exons and splice junctions of *GAS2L2* and to amplify the breakpoint of the large deletion in *GAS2L2*

Position	Primers (5'-3')
Exon 1	F: ACACGGGAACCTCAGAATCA
	R: CCAGAGCTAGCCTGTGCATT
Exon 2	F: GAGGCTCAGGTCCTCTGG
	R: AAGGGGGTGGGTTAGTGG
Exon 3	F: AGAAACCTCAGGGGTGACCT
	R: CATATTCTGGGAGACTTAGTGTCATT
Exon 4	F: TGGGTACATGGATGAGAGCA
	R: GACATACCTCCCACCTCTGC
Exon 5	F: TTGCCACTGTAGGTCCCACT
	R: CCGAGGATCTGCTCCTTTTA
Exon 5	F: GTGTTGCCACTGTAGGTCCC
	R: GTCTCGGGGTAGAGGCACTG
Exon 6	F: CCGGCCTGATGAGTCTCC
	R: GCCAGGTCCACAGTGACG
Intron 4	F: GTGTTGCCACTGTAGGTCCC*
RAS10LB 3'UTR	R: AGCGGATGAAGGATGGCAGC*

*: Primers used to amplify the breakpoint of the large deletion in *GAS2L2* [c.867_*343+1207del]

TableS3: Primers used for human (h), mouse (m), and morpholinos sequence

Primers used for RT-PCR

Name	Primer Sequence	PCR Product Size (bp)
h *GAS2L2*	F: TACCTTCCAGGCCAGGGACAAT	309
	R: ATCTGGTCCAGGTTGCGGAAGT	
h *GAS2L2*	F: TGGGACACACTGGGCCATTA	685
	R: CCCTGAACTGGAAGAACGCA	
h PPIA	F: CCGTGTTCTTCGACATTGCC	371
	R: ACACCACATGCTTGCCATCC	
h DNAI1	F: AGAGAAGGAGAAGGCAAAGACCCC	401
	R: TGTACTCAGGGAAGCTGGGGTTCT	
m Gas2l2	F: ATGTCTCAGCATGTGGGACA	537
	R: GCAGCTCCTCATCAATTTCC	
m Tbp	F: GCCTTCCACCTTATGCTCAG	200
	R: TACTGCCTGCTGTTGTTGCT	
m Actin	F: CATCACTATTGGCAACGAGC	283
	R: GATCCACACAGAGTACTTGC	

Primers used for Genotyping

Genotype	Primer Sequence	PCR Product Size (bp)
m Gas2l2$^{+/+}$ *and m Gas2l2*$^{+/-}$	F: CAGGAGCAGGTGAGTATTTGGAGC	264
	R: GGTCACATAGCCACAGGAGATT	
m Gas2l2$^{+/-}$ *and m Gas2l2*$^{-/-}$	F: CAGGAGCAGGTGAGTATTTGGAGC	365
	R: TCGTGGTATCGTTATGCGCC	
m Gas2l2^{flox}	F: CGAAGTTATGTCGAGATATCTAG	604
	R: GCAGCTCCTCATCAATTTCC	
m Gas2l2 targeted/ deleted	F: GATGGGAAGGAAGCTCAAGGCG	wt: 2009
	R: GACCATGGAGAATTGCACTGGG	targeted: 2090
		deleted: 1139
GFP	F: CCACAAGTTCAGCGTGTCC	487
	R: GGT GTT CTG CTG GTA GTG G	
Cre	F: GCGGTCTGGCAGTAAAAACTATC	100
	R: GTGAAACAGCATTGCTGTCACTT	

Morpholinos

Gas2l2 **isoform 1**	CACTG CCACCCTGATGAGTTGACAT
Gas2l2 **isoform 2**	GAGCTATACACATACACCTTCCAGA

TableS4: Primary Antibodies

Antibody Name	host	company	Catalog#	dilution WB	dilution IF	dilution SR
GAS2L2	rabbit	Atlas	HPA044370	1:1000	1:500	1:1000
GAS2L2	mouse	Sigma	SAB1412937	1:1000	1:500	1:1000
CROCC	rabbit	Atlas	HPA021191	NT	1:500	1:1000
EB1	rabbit	Atlas	HPA003600	1:1000	1:500	1:1000
EB3 (KT36)	rat	Absea	010314H04	1:1000	1:500	1:1000
ERICH3	goat	Santa Cruz BT	discontinued	NT	1:250	NT
CENTRIN-2	rabbit	Atlas	HPA045880	NT	1:250	1:500
Acetylated-α TUBULIN	mouse	Sigma	T7451	NT	1:1000	NT
γ-TUBULIN	mouse	Sigma	T6557	1:1000	1:500	1:1000
γ-TUBULIN	rabbit	Biolegend	620901	NT	1:250	NT
CENTRIOLIN (C-9)	mouse	Santa Cruz BT	SC-365521	NT	1:250	NT
MUC5B (H-300)	rabbit	Santa Cruz BT	SC-20119	NT	1:500	NT
CC10 (E11)	mouse	Santa Cruz BT	SC-365992	NT	1:250	NT
ACTIN	mouse	Thermo Fisher	MA511869	1:5000	1:500	1:1000

NT: not tested

Table S5: Demographic, clinical phenotype and *GAS2L2* genetic variants in 2 PCD-affected individuals from 2 unrelated families

								Allele 1			Allele 2		
Family	**PCD #**	**Sex**	**Age (yrs)**	**Ethnicity**	**nNO (nl/min)**	**Ciliary structure**	**Other Clinical features**	**Exon/ Intron**	**Genetic variant**	**Protein variant**	**Exon/ Intron**	**Genetic variant**	**Protein variant**
UNC-362	1367 (2-VI)	M	56	Caucasian	342.6[a]	Normal	NRD: No Bxsis sinusitis Otitis media Situs Status: SS Infertile	Ex 5	c.887_890del TAAG	p.(Val296Glyfs*13)	Ex 5	c.887_890del TAAG	p.(Val296Glyfs*13)
DC-630	DCP-1040 (2-I)	F	11	Caucasian	47[b]	Normal	NRD: No Bxsis sinusitis Otitis media Situs Status: SS Fertility: ND	Ex 5	c.887_890del TAAG	p.(Val296Glyfs*13)	Large del	c.867_*343+1207 del	p.?

Abbreviations: M, male; F, female; nNO, nasal nitric oxide; NRD, neonatal respiratory distress; Bxsis, bronchiectasis; SS, *situs* solitus; ND, not determined; Ex, exon; del, deletion.

[a] cutoff value of 77nl/min[11]

[b] cutoff value of 82.2 nl/min[12]

Table S6: Dot product scores for the peptides selected for GAS2L2 targeted proteomics in the analyzed bands.

Peptides chosen for PRM	GAS2L2 overexpressed	Deciliated cells high band	Deciliated cells low band	H. Nasal *GASL2*$^{-/-}$ high band	H. Nasal *GASL2*$^{-/-}$ low band
K.SSEQYLEA**M**KEDLAEWLR.D [25, 42] (missed1)	0.97*	0.77	0.65	0.72	0.66
R.VGVS**C**NGAAQPGTFQAR.D [94, 110]	0.98*	0.78	0.94*	0.51	0.86
R.DNVSNFIQW**C**R.K [111, 121]	0.99*	0.98*	0.76	0.5	0.78
R.VGDSNTLIFIR.I [234, 244]	0.95*	0.82	0.92*	0.46	0.51
R.VQDGPSQTQPTMTISR.S [297, 312]	0.97*	0.97*	0.84	0.67	0.56
R.IPTSWVHEETDSWGTDAGNPTPQR.L [415, 438]	0.99*	0.97*	0.77	0.72	0.56

Peptide Key: (flanking residue).(Sequence).(flanking residue) [position in protein] (# missed cleavages, if any)
M = oxidized methionine
C = carbamidomethyl cysteine
*: The dot product score > 0.9 is considered a valid ID[13]

SUPPLEMENTAL METHODS

Targeted proteomic analysis

Cell cultures were deciliated[14]. Following deciliation, the cell body fraction was lysed as described in main text. For proteomics analysis, samples were loaded onto 4−12% Nu-PAGE gradient gels (Novex) for separation. For targeted proteomics 2 sections were cut from each lane; one containing proteins between 80-120 kDa and one containing proteins between 25-45 kDa to detect peptides associated to full length and a possible truncated form of GAS2L2, respectively. Each section was subjected to in-gel trypsinization [15]. In-gel digests were separated by automated nanoflow liquid chromatography coupled to tandem mass spectrometry (LC-MS/MS) using a Thermo Easy nLC 1000 coupled to a QExactive HF mass spectrometer. First, a positive control (over-expressed GAS2L2-Halo tag) was analyzed in data-dependent acquisition (DDA) mode on the QExactive HF, where the 15 most abundant peptides were chosen for HCD fragmentation. Raw data were searched against a reviewed human Uniprot database using Sequest within Proteome Discoverer (Thermo, version 2.1) and only peptides with a false discovery rate (FDR) of ≤5% were further considered. Next, the full length and possible truncated GAS2L2 samples were analyzed using the QExactive HF in parallel reaction monitoring (PRM) mode to enhance selectivity and sensitivity [16]. Peptides were chosen from the DDA analysis based on location in the GAS2L2 sequence (between amino acid 25 and 438), quality of spectra, and scores. The target list for the PRM method included m/z as well as retention times (each target peptide should elute at the same time from sample to sample). The PRM method parameters were as follows: resolution set to 15,000; AGC target, 5e5; Maximum IT, 500 ms; and isolation window, 2 m/z. Skyline software was used

to compare the peptide PRM data acquired for GAS2L2 over-expressed (positive control) with the PRM data acquired for the high and low molecular weight gel slices from the *GAS2L2* deficient (PCD-1367) samples.

B-Galactosidase staining

Tissues from adult male and female *Gas2l2*$^{+/-}$ mice were dissected and frozen in OCT on dry ice. The frozen block was sectioned at 10 µm. The sections were fixed in cold 0.2% glutaraldehyde, 5mM EGTA, 2mM $MgCl_2$ in PBS pH7.4 for 10 min at room temperature. Samples were washed with wash solution: 0.1 M phosphate buffer pH 7.4, supplemented with 2 mM $MgCl_2$, 0.01% Sodium deoxycholate and 0.02% NP-40, 3 times for 5 min. Samples were immersed in staining solution (washing solution containing: 2 mg/ml X-gal ([5-bromo-4-chloro-3-indolyl-β-D-Galactopyranoside; Cayman Chemical Co. #16495] stock 50 mg/ml in dimethylformamide), 5mM $K_3Fe(CN)_6$, $K_4Fe(CN)_6$ (Sigma) and incubated over night at room temperature in the dark. The next day slides were washed with wash solution 3 x 5 min. Samples were counter-stained with 1% nuclear fast red for 30s and thoroughly washed in water. Samples were dehydrated and mounted with Permount. Images were taken with an Olympus VS120 virtual slide Scanner microscope.

REFERENCES

1. Zariwala, M.A., Knowles, M.R., and Leigh, M.W. (2007 [Updated 2015]). Primary Ciliary Dyskinesia. In GeneReviews(R), R.A. Pagon, M.P. Adam, H.H. Ardinger, S.E. Wallace, A. Amemiya, L.J.H. Bean, T.D. Bird, N. Ledbetter, H.C. Mefford, R.J.H. Smith, et al., eds. (Seattle (WA), University of Washington, Seattle; 1993-2017
2. Hoben, I.M., Hjeij, R., Olbrich, H., Dougherty, G.W., Nothe-Menchen, T., Aprea, I., Frank, D., Pennekamp, P., Dworniczak, B., Wallmeier, J., et al. (2018). Mutations in C11orf70 Cause Primary Ciliary Dyskinesia with Randomization of Left/Right Body Asymmetry Due to Defects of Outer and Inner Dynein Arms. American journal of human genetics 102, 973-984.

3. Fassad, M.R., Shoemark, A., le Borgne, P., Koll, F., Patel, M., Dixon, M., Hayward, J., Richardson, C., Frost, E., Jenkins, L., et al. (2018). C11orf70 Mutations Disrupting the Intraflagellar Transport-Dependent Assembly of Multiple Axonemal Dyneins Cause Primary Ciliary Dyskinesia. American journal of human genetics 102, 956-972.
4. El Khouri, E., Thomas, L., Jeanson, L., Bequignon, E., Vallette, B., Duquesnoy, P., Montantin, G., Copin, B., Dastot-Le Moal, F., Blanchon, S., et al. (2016). Mutations in DNAJB13, Encoding an HSP40 Family Member, Cause Primary Ciliary Dyskinesia and Male Infertility. The American Journal of Human Genetics 99, 489-500.
5. Olbrich, H., Cremers, C., Loges, N.T., Werner, C., Nielsen, K.G., Marthin, J.K., Philipsen, M., Wallmeier, J., Pennekamp, P., Menchen, T., et al. (2015). Loss-of-Function GAS8 Mutations Cause Primary Ciliary Dyskinesia and Disrupt the Nexin-Dynein Regulatory Complex. American journal of human genetics 97, 546-554.
6. Bonnefoy, S., Watson, C.M., Kernohan, K.D., Lemos, M., Hutchinson, S., Poulter, J.A., Crinnion, L.A., Berry, I., Simmonds, J., Vasudevan, P., et al. (2018). Biallelic Mutations in LRRC56, Encoding a Protein Associated with Intraflagellar Transport, Cause Mucociliary Clearance and Laterality Defects. American journal of human genetics 103, 727-739.
7. Olcese, C., Patel, M.P., Shoemark, A., Kiviluoto, S., Legendre, M., Williams, H.J., Vaughan, C.K., Hayward, J., Goldenberg, A., Emes, R.D., et al. (2017). X-linked primary ciliary dyskinesia due to mutations in the cytoplasmic axonemal dynein assembly factor PIH1D3. 8, 14279.
8. Paff, T., Loges, N.T., Aprea, I., Wu, K., Bakey, Z., Haarman, E.G., Daniels, J.M.A., Sistermans, E.A., Bogunovic, N., Dougherty, G.W., et al. (2017). Mutations in PIH1D3 Cause X-Linked Primary Ciliary Dyskinesia with Outer and Inner Dynein Arm Defects. The American Journal of Human Genetics 100, 160-168.
9. Edelbusch, C., Cindric, S., Dougherty, G.W., Loges, N.T., Olbrich, H., Rivlin, J., Wallmeier, J., Pennekamp, P., Amirav, I., and Omran, H. (2017). Mutation of serine/threonine protein kinase 36 (STK36) causes primary ciliary dyskinesia with a central pair defect. Human mutation 38, 964-969.
10. Wallmeier, J., Shiratori, H., Dougherty, Gerard W., Edelbusch, C., Hjeij, R., Loges, Niki T., Menchen, T., Olbrich, H., Pennekamp, P., Raidt, J., et al. (2016). TTC25 Deficiency Results in Defects of the Outer Dynein Arm Docking Machinery and Primary Ciliary Dyskinesia with Left-Right Body Asymmetry Randomization. The American Journal of Human Genetics 99, 460-469.
11. Leigh, M.W., Hazucha, M.J., Chawla, K.K., Baker, B.R., Shapiro, A.J., Brown, D.E., LaVange, L.M., Horton, B.J., Qaqish, B., Carson, J.L., et al. (2013). Standardizing Nasal Nitric Oxide Measurement as a Test for Primary Ciliary Dyskinesia. Annals of the American Thoracic Society 10, 574-581.
12. Beydon, N., Chambellan, A., Alberti, C., Blic, J.d., Clément, A., Escudier, E., and Bourgeois, M.L. (2015). Technical and practical issues for tidal breathing measurements of nasal nitric oxide in children. Pediatric pulmonology 50, 1374-1382.
13. Yen, C.-Y., Houel, S., Ahn, N.G., and Old, W.M. (2011). Spectrum-to-Spectrum Searching Using a Proteome-wide Spectral Library. Molecular & cellular proteomics : MCP 10, M111.007666.
14. Blackburn, K., Bustamante-Marin, X., Yin, W., Goshe, M.B., and Ostrowski, L.E. (2017). Quantitative Proteomic Analysis of Human Airway Cilia Identifies Previously Uncharacterized Proteins of High Abundance. Journal of proteome research 16, 1579-1592.
15. Wilm, M., Shevchenko, A., Houthaeve, T., Breit, S., Schweigerer, L., Fotsis, T., and Mann, M. (1996). Femtomole sequencing of proteins from polyacrylamide gels by nano-electrospray mass spectrometry. Nature 379, 466.

16. Gallien, S., Bourmaud, A., Kim, S.Y., and Domon, B. (2014). Technical considerations for large-scale parallel reaction monitoring analysis. Journal of Proteomics 100, 147-159.